A STUDY ON GEOMETRICAL PARAMETERS INFLUENCING THE MECHANICAL SPREADING OF FIBRE BUNDLES

M. Tonejc[1], H. Steiner[2], E. Fauster[2], S. Konstantopoulos[1] and R. Schledjewski[1, 2]

[1]Christian Doppler Laboratory for High Efficient Composite Processing, Montanuniversität Leoben,
OttoGlöckel-Strasse 2/1, 8700 Leoben, Austria
Email: maximilian.tonejc@unileoben.ac.at, web page: http://www.kunststofftechnik.at/lvv-cdl-en/

[2]Chair of Processing of Composites, Department Polymer Engineering and Science, Montanuniversität Leoben
OttoGlöckel-Strasse 2/3, 8700 Leoben, Austria
Email: ralf.schledjewski@unileoben.ac.at, web page: http://www.kunststofftechnik.at/composites/

Keywords: fibre spreading, spreading parameters, continuous impregnation, fibre placement, filament winding

ABSTRACT

For composites manufacturing processes such as automated fibre placement, filament winding or pultrusion, roving behaviour is crucial. Understanding and controlling these processes is only possible if material changes induced by guidance to the processing area are fully understood. Fibre placement system manufacturers such as Coriolis Composites use a creel to store and feed material to a placement head. Material deflection take place in the creel system as well as in the placement head itself, which unintentionally can impact the material prior to being processed.

In this work, a two-stage-approach is presented to address the topic of roving spreading properties for future application in guidance optimization. In the first phase, a manual spreading test rig was set up. It consists of three rollers whose position form an isosceles triangle on a rigid composition of aluminium profiles. The specimen used for the experiments were pre-cut, clamped to weights, measured in dimensions and applied to the setup. Through geometrical alterations in the setup, changes in spreading behaviour were observed and put into context with an existing spreading model developed by Wilson [1]. As a result, the lateral changes in width were studied in manifolds of three back-and-forth motions until equilibrium of spreading was achieved.

In the second phase, a configuration of five acetal rollers was set up on an automated spreading test rig. The used material was taken off continuously from a spool fixed on a mandrel. The roving was then initially measured in its cross-sectional dimensions by means of light sectioning sensor, then guided through the configuration of rollers and finally profiled again. An emphasis in this phase was put on the systematics to acquire profiling data and influences corrupting the experiments.

1 INTRODUCTION

A significant portion of fibre-reinforced polymer composite parts is fabricated by means of continuously running processes such as fibre placement, filament winding or pultrusion. These processing techniques share the need for continuous impregnation techniques, where the reinforcing fibres are impregnated with the liquid matrix material. Obviously, this processing step is crucial for the quality of the final composite part.

Considering composites with either thermoset or thermoplastic resin based matrix materials, four major groups of continuous impregnation techniques are well established: powder impregnation, hot melt impregnation, solution impregnation and methods based upon commingled yarns. One thing all of these methods have in common is the need of understanding fibre bundle's spreading behaviour under different conditions. To ensure full material saturation for processes such as pultrusion, different spreading methods are well established e.g. methods based upon vacuum, compressed air, vibration or form of deflection [2]. First mentioned methods put a heavy emphasis on spreading for subsequent through thickness impregnation [3–6].

In contrast, spreading through form and deflection is also applied on research to study micro and macro behaviour of dry, fully impregnated or partially impregnated rovings [1, 7, 8] which finds its application in processes such as Automated Tape Placement, Automated Fibre Placement and Automated Dry Fibre Placement. In these processes material, either fully or partially impregnated, is guided through a placement head, then cut, heated and placed on an open mould [1, 9–11]. Due to the mechanical properties of the individual placement systems the processed material has to withstand different states of stress. Hence it is likely that the dimensions of the virgin material change through processing before being placed on the mould.

In this work, a two phase approach to investigating bindered rovings was evaluated. Therefore in the first phase a manual test rig was setup to approve the predicted behaviour after Wilson's Model [1]. In the second phase a setup on an automatized test rig was realized to investigate material behaviour with respect to process conditions.

2 MECHANICAL SPREADING MODEL

In the first phase of tests the mechanical spreading model of Wilson [1] was taken as reference for investigating the fibre bundle spreading behaviour. A slight variation of Wilson's original test setup is shown in Figure 1. Wilson achieved spreading of filaments through back-and-forth motions until an equilibrium stage in spreading was reached. Subsequent to these reciprocal motions, the width of the fibre bundle was measured at the upper rod.

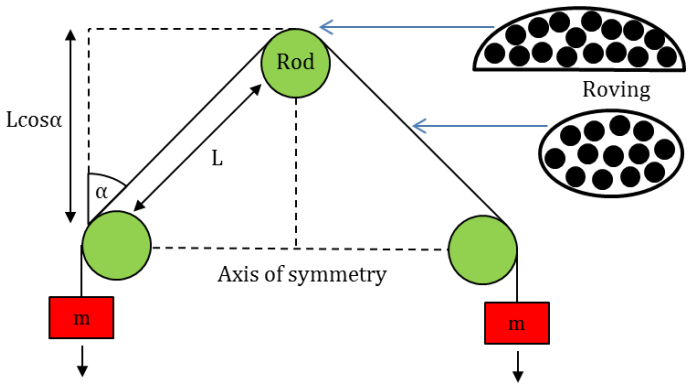

Figure 1: A schematic of Wilson's test setup.

Wilson treated fibre bundles as a continuum and derived a correlation between the bundles width and thickness depending on pure geometrical factors and no dependencies on stress. The width (W) of the bundle and the thickness (t) on top of the upper rod were predicted as:

$$\mathrm{W} = (12\mathrm{AL}\cos\alpha)^{1/3}\,, \tag{1}$$

$$t = \left(\frac{9A^2}{32L\cos\alpha}\right)^{1/3} \tag{2}$$

where A [mm^2] displays the cross-sectional area of the bundle, L [mm] the free length between deflections and α the angle between the vertical axis and the fibre bundle. The term '$\mathrm{L}\cos\alpha$' was treated as a single parameter since there seems to be a strong dependency lying within. Originally Wilson's experiment focused on the behaviour of polyamide fibres investigating bundles consisting of 10^5 filaments at an average diameter of $23\mu m$ [1, 7].

3 EXPERIMENTAL WORK

3.1 Materials

The materials used in the tests were supplied by Exel Composites GmbH and Toho Tenax Europe GmbH, respectively.

Exel Composites GmbH provided a StarRov 086 direct E-glass roving produced by Johns Manville with $4800tex$, a filament diameter of $23\mu m$ and an approximate number of 4000 filaments. The roving was carefully drawn from the centre of the bobbin and placed on a workbench where it was untwisted until no more twists were observed in the material. It was then used for the experiments on the manual spreading test rig. After several pre-trails a free clamping length of $1.7m$ was chosen to be appropriate for a measurement length of $300mm$ in the middle of each specimen. More detailed information can be found in Section 4. Due to the sizing of roving, twists and dimensional inconsistencies were observed as one can see in Figure 2.

Figure 2: Detailed view on the StarRov 086 direct E-glass roving covering a length of approximately 50mm .

Toho Tenax Europe GmbH provided the Tenax-E HTS40 F13 direct carbon roving with $1600tex$ and $24K$. It was used at the automated test rig where it was directly unwound from the spool to the test rig.

3.2 Manual Spreading Test Rig

The setup depicted in Figure 1 was realized utilizing aluminium profiles as shown in Figure 3 (left). Compared to Wilson's original test setup, acetal rollers were used instead of rods. Those custom made rollers are available in diameters of $20mm$, $30mm$ and $40mm$, consisting of an acetal body with a shaft hole, ball bearings and a shaft. The shaft of each roller was clamped in a bracket guided in a linear groove. Thus, the rollers can be adjusted relatively in height to each other. The horizontal distance of two parallel grooves was given with $120mm$.

For the tests two different weights were selected and connected to both ends of the roving. Therefore two different series of tests at stress levels induced with $0.5kg$ at each end or $1.25kg$ were performed. The rovings were knotted to the weights on the workbench and then carefully transferred to the test rig. Then the roving was measured in width and thickness with a sliding calliper every $20mm$ of the measurement length.

Figure 3: Test setup for manual spreading (left) and knot to connect the fibre bundle to the stress inducing weights (right).

After determining the initial dimensions of the roving, back-and-forth motions (later referred as reciprocal motions) were performed with a manifold of three (Figure 4). Depending on the lateral moving behaviour of the roving, different stages of reciprocal motions could be achieved. After each set of three reciprocal motions the roving was once again measured in width at the same points likewise the initial measurement. To assure catching the same points each time the marked ends of the testing length on the roving as well as a yarn that had equidistant $20mm$ marks were matched. Usually the number of 12 reciprocal motions was exceeded up to a maximum number of 24 reciprocal motions.

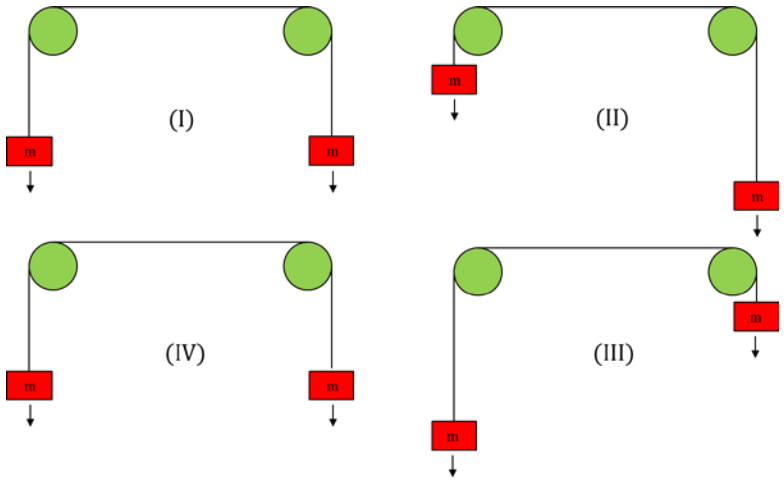

Figure 4: A schematic showing one reciprocal motion [7] – order from (I) to (IV).

Besides varying weights, different '$L\cos\alpha$' values were realized through moving the centre roller vertically in the groove. Four test rig adjustments were investigated and are displayed in Figure 5. Therefore L was selected at $150mm$, $200mm$, $250mm$ and $300mm$ and the angles were $53°$, $37°$, $29°$ and $23°$.

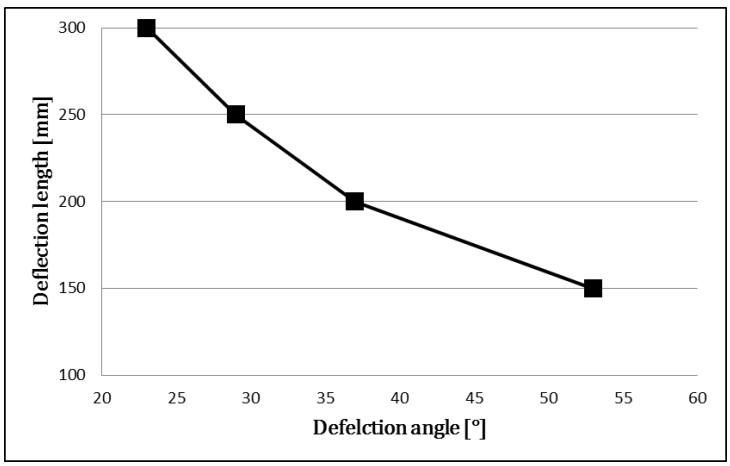

Figure 5: Correlation between L and α at the given horizontal distance of $120mm$ between the aluminium profiles.

3.3 Automated Spreading Test Rig

For the second phase a test rig was set up consisting of different actuators and sensors controlling and monitoring the process as displayed in Figure 7. The goal of this test rig was to create an environment for continuous spreading tests. Compared to the manual spreading test rig where the specimens were pre-cut, untwisted and clamped 'offline', the automated test rig held the full spool of material on the unwinding mandrel and material was pulled out continuously.

To minimize the incoming angle of the roving the unwinding mandrel was placed in $5m$ distance to the linear guidance. Therefore a very sensitive aspect of the test, namely the profiling step could be better controlled. Moreover the rovings tendency to wrinkle under stress and twist was limited through the extended distance of the mandrel. Due to the optical design of the light sectioning sensor a narrow window had to be selected to achieve sufficient resolution of the roving's surface. Detailed information can be found in the results section. Finding a balance between sufficient contrast and minimized reflections a shutter time between $40ms$ and $70ms$ was selected guaranteeing 3 to 5 fps acquisition rate. Furthermore, the roving was guided over a cylindrical surface that was covered with a tape ensuring a diffuse surface as shown in Figure 6. For evaluating the measurement data, a Matlab tool was used for the automated spreading test rig. The tool will be further described in the results section of the paper. The distance between the incoming measurement point and the outlet point for the second measurement was $1.1m$ for values for L of $150mm$ and α of 53°.

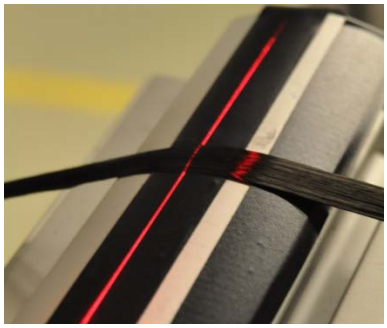

Figure 6: Illustration of the light sectioning used for roving profiling.

After measuring the virgin width the roving was guided under and over five acetal rollers to achieve spreading. This was continued for $1.1m$ until the first incoming point reached the outlet point where the roving was measured in profile for a second time.

The latter sensors on the test rig displayed the acting force which was set to approximately $70N$ and the actual velocity that was set to $30mm/s$.

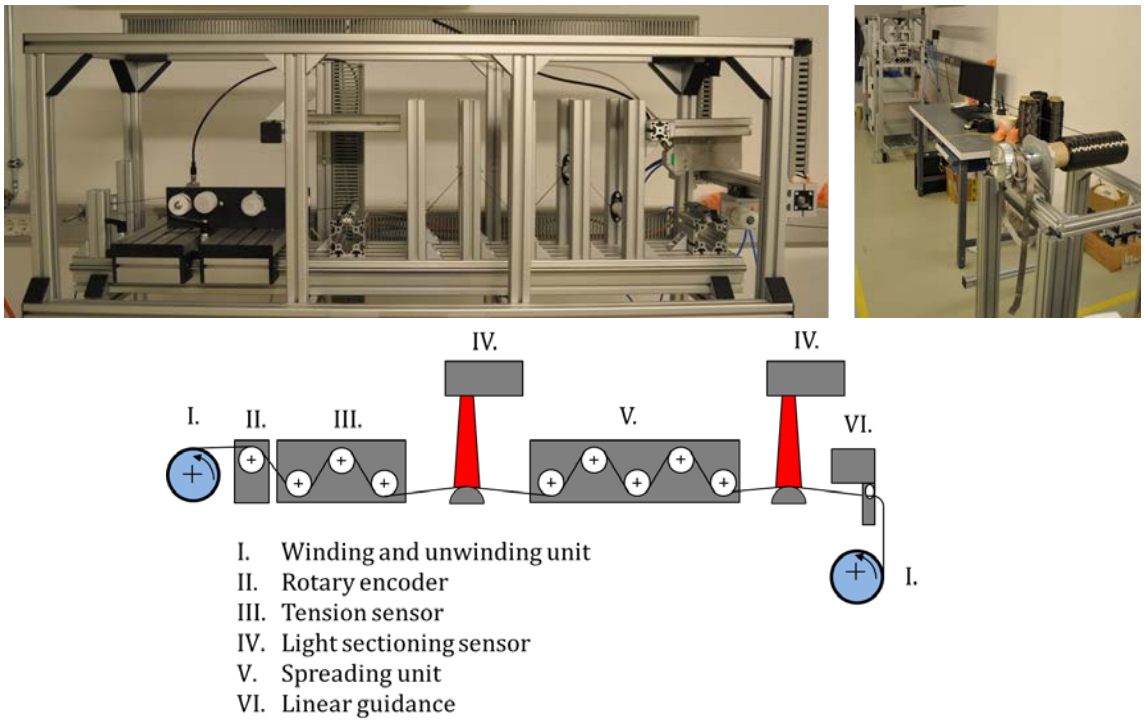

Figure 7: Test setup (top row pictures) and schematic of the automated spreading test rig (lower illustration).

3.4 Manual Spreading Results

In this section, selected results are presented that show behaviour in general during the manual spreading tests. Acting as an example values for L of 250mm and α of 29° was selected due to its significant characteristics. The displayed results are put into relation to the original width of the roving in percentage as described in:

$$S = \frac{width_{spread}}{width_{virgin}} * 100\ (\%) \tag{3}$$

In Figure 8 a series of experiments with 0.5kg as applied weight is displayed. The most noticeable issue is that specimen 2 shows a much higher spreading behaviour than specimen 1 and 3. This effect might be correlated to an inhomogeneous sizing application but needs to be further investigated. The highest occurring spreading was observed at specimen 2 with a value of 167% while the highest average value of all three specimens is 135%. The spreading predicted by the model of Wilson is 224% which leaves a difference of 89%. Another noticeable fact is the high error within a single experiment as well as over all three experiments. The error observed lies between 11% and 33% for this series of experiments.

In comparison, Irfan [7] observed in general higher spreading rates than predicted by the model of Wilson while reporting significant amounts of error as well. That leaves the question where this discrepancy is rising from. One explanation is the type of alteration performed in the experiments of our study. In contrast to Wilson or Irfan, acetal rollers were used instead of rods. Undoubtedly this decreases the amount of friction between the outer filaments of the fibre bundle and the deflection surface and therefore the state of stress acting on the fibre bundle. Another reason for the high discrepancy is owed to the different measurement of the virgin width. While Irfan was measuring the fibre bundle 'offline' on the workbench without any applied stress, this study was measuring the virgin width on the test rig just before the experiments were started. Thereby dimensional differences might have occurred. None the less the authors of this study think that it is more sufficient to collect dimensional data directly on the test rig due to the non-uniformity of this particular material (Figure 2).

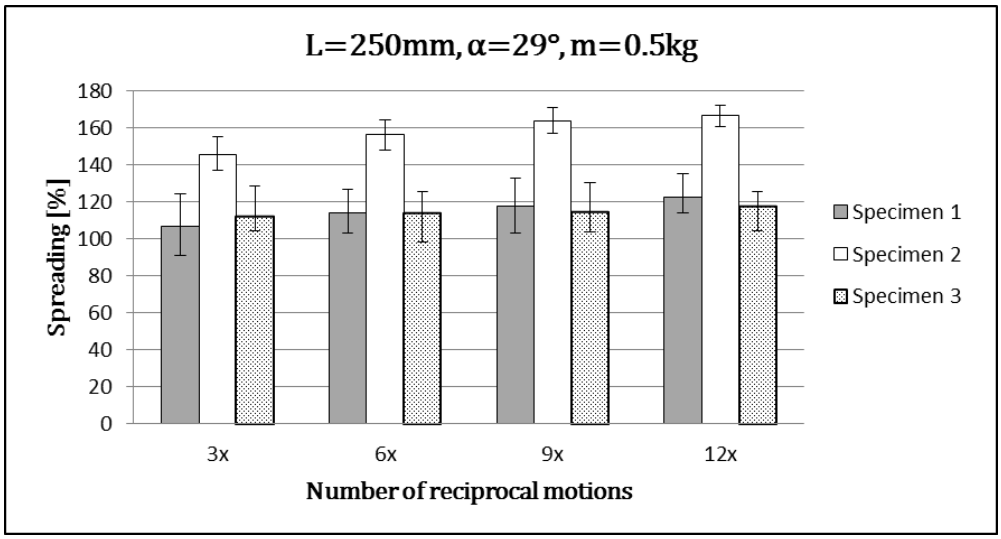

Figure 8: Average spreading of a series of specimens at a discrete 'L cos α' of 250mm and 29° with weights of 0.5kg applied.

In Figure 9 a series of experiments with 1.25kg of applied weights is displayed. As one can notice, compared to Figure 8 the overall behaviour of specimen 1 to 3 is a lot more uniform. Furthermore a higher number of reciprocal motions were performed. This is due to the fact that higher weights seem to have an influence on lateral movement on the rollers. Moreover it is slightly noticeable that the error decreased to values between 11% and 28%. The maximum spreading within the series of

experiments was 156% and the maximum average spreading was 154%. But again Wilson's model predicted much higher spreading than observed, expected to be about 211%.

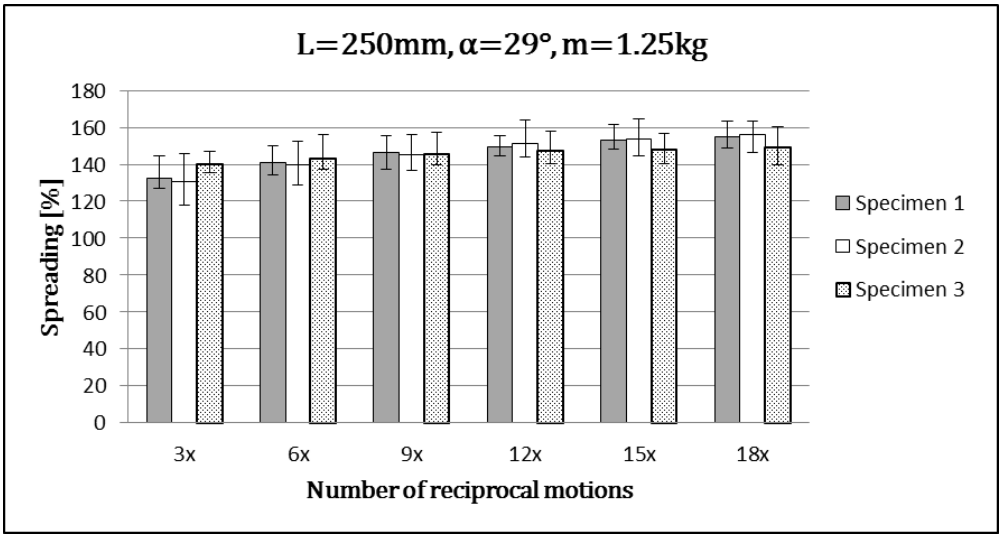

Figure 9: Average spreading of a series of specimens at a discrete '$L\cos\alpha$' of 250mm and 29° with weights of 1.25kg applied.

In Figure 10 a compilation of all experiments for $0.5kg$ and $1.25kg$ are displayed. There all experiments at the same weight, independent of '$L\cos\alpha$' were averaged for the different stages of reciprocal motions. Since this data representation covers such a vast field of experimental conditions, error bars were excluded; none the less different behaviour can be observed. One can see that the overall spreading 'willingness' decreases with the amount of weight applied. That contradicts the assumption of Wilson [1] who stated that the mechanical spreading is independent of stress applied.

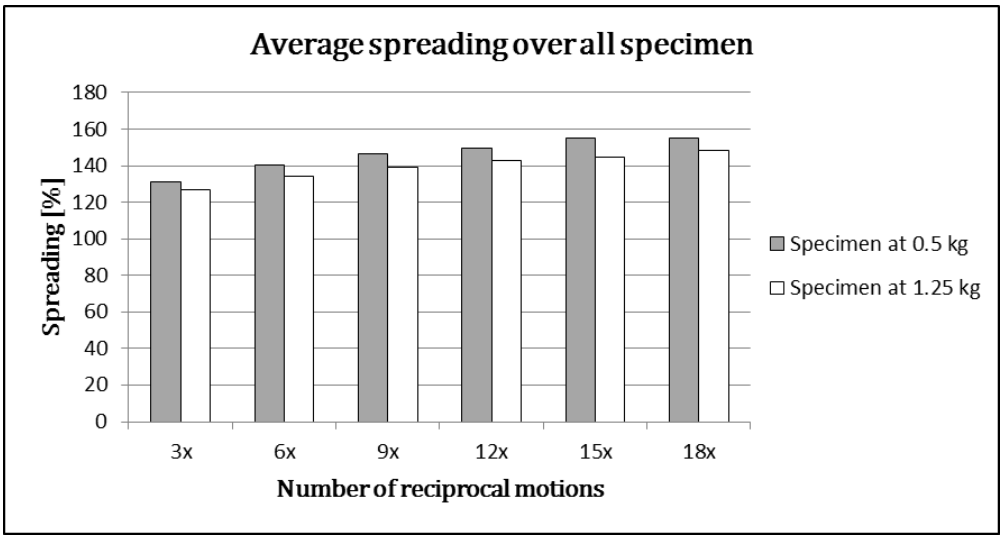

Figure 10: Average spreading of discrete weights over all '$L\cos\alpha$' values.

3.5 Automated Spreading Results

In this section selected results are presented for the automated spreading test rig. The geometrical parameters for '$L\cos\alpha$' were 150mm and 53°. Since spreading was insufficient, an emphasis is put on the method for acquiring profiling data and error influences in the experiments.

In Figure 11 an exemplary comparison between a virgin roving's profile and a spread roving's profile is displayed. This particular time stage of one experiment shows a spreading of 114% calculated using Equation (3) while the average spreading of this experiment was 110%. The average

thickness of the virgin roving was $0.287mm$, then decreased due to spreading and consequently thinned to $0.227mm$. This corresponds to a decrease of 21% in thickness resulting in a cross-sectional areal loss of 16%.

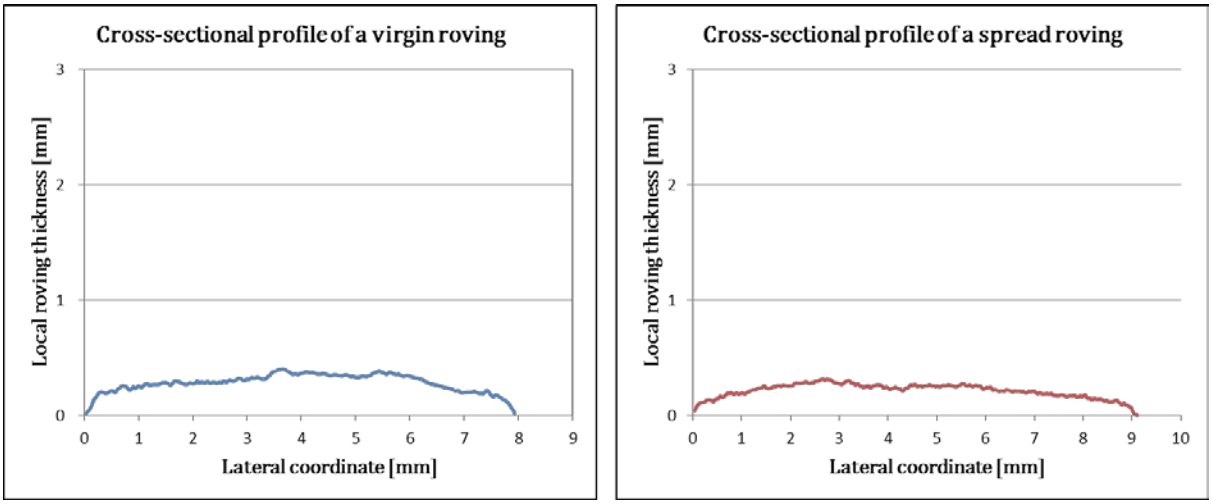

Figure 11: Comparison of a virgin roving (left) and a spread roving (right) in a cross-sectional view, recorded via light sectioning.

In Figure 12 the unprocessed experiment data is displayed. As one can notice the profile consists of a higher number of data points and also seems to be tilted in comparison to Figure 11. The Matlab program is basically fulfilling the following tasks:

1 filter error data points such as ripped fibres or optical flaws,
2 tilting the profile into the horizontal level,
3 shift the profile into the zero level of thickness,
4 detect the edges of the roving through a threshold value given by the user,
5 extract the pure profile data points,
6 determine values for thickness, width and cross-sectional area and export the data.

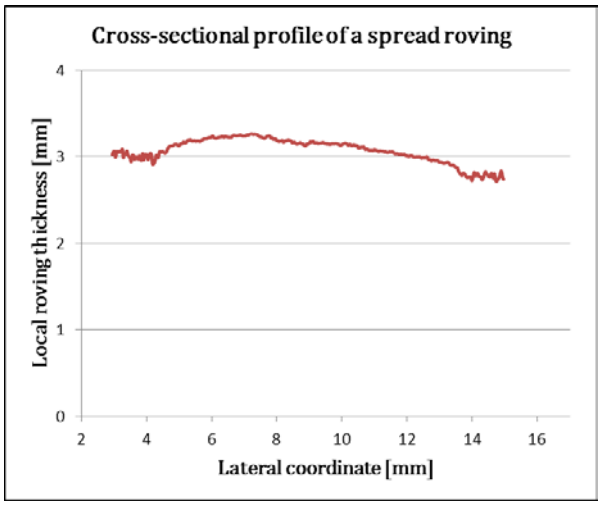

Figure 12: Original unprocessed data acquired with the light sectioning sensor.

What has been noticed during the experiments was that the sizing of the carbon fibre sometimes produces reflections that induce optical flaws that later need to be filtered or even corrupt the whole experiment. Also a very narrow test window needs to be selected to avoid unpleasant optical influences that compromise the algorithm to work properly. Therefore many experiments needed to be neglected due to data corruption or reflections.

4 CONCLUSIONS

In this work, two approaches investigating fibre bundle spreading were presented. In the first phase of experiments a modified test setup of Wilson was used to monitor fibre spreading via deflections induced through acetal rollers. This approach was chosen out of two reasons. First, it was reported by Irfan [7] that glass rovings but especially direct carbon rovings tend to be damaged by rods when the deflection number increases. Second, it seemed more convenient to the authors using rollers since further investigations will address roving behaviour in processes such as Automated Dry Fibre Placement of Filament Winding. None the less it was clearly observed that utilizing rollers showed a decrease in the overall spreading behaviour predicted by Wilson [1]. Also reasons for the high deviations between experiments need to be addressed. A possible influence could derive from the inconsistencies of sizing application on the roving. Besides, a different method like light sectioning needs to be applied on the manual test setup to reach a sufficient level of profiling since measuring with a sliding calliper for sure induced extra human error.

In the second phase, experiments on the automatized spreading test rig were carried out. An emphasis was put on the method of measuring and the post processing of the data. The overall spreading behaviour was very low. Nevertheless, adaptations for further experiments are foreseen concerning the linear guidance as well as the surface material for optical data acquisition. This test rig will be utilized in future works to investigate roving behaviour in complex placement systems and characterize unintentional spreading behaviour of such systems by combining steady deflections (rods) and “friction free” (rollers).

ACKNOWLEDGEMENTS

The authors kindly acknowledge the financial support received from the “Bundesministerium für Wissenschaft, Forschung und Wirtschaft” as well as the “FACC Operations GmbH” in frame of the “Christian Doppler Laboratory for High Efficient Composite Processing”.

REFERENCES

[1] S. Wilson, Lateral spreading of fibre tows, *Journal of Engineering Mathematics,* **32**, 1997, pp. 19–26 (doi: 10.1023/A:1004253531061).

[2] C. Zaniboni, Oligomere Technologies for Cost-Effective Processing High-Performance Polyphthalamide Composites, Diss. ETH Zürich, 2010.

[3] H. EL-Dessouky and C. Lawrence, Ultra-lightweight carbon fibre/thermoplastic composite material using spread tow technology, *Composites: Part B,* **50**, 2013, pp. 91–97 (doi: 10.1016/j.compositesb.2013.01.026).

[4] N. Nakagawa and Y. Ohsora, Fiber separator for producing fiber reinforced metallic or resin body, EP Patent 0,393,420, 1993.

[5] R. Krueger, Apparatus and method for spreading fibrous tows into linear arrays of generally uniform density and products made thereby, US Patent 6,311,377, 2001.

[6] K. Kawabe, H. Sasayama and S. Tomoda, New Carbon Fiber Tow-Spread Technology and Applications to Advanced Composite Materials, *SAMPE journal 45*, 2009, pp. 6–17.

[7] M. Irfan, V. Machavaram, R. Mahendran, N. Shotton-Gale, C. Wait, M. Paget, M. Hudson and G. Fernando, Lateral spreading of a fiber bundle via mechanical means, *Journal of Composite Materials,* **3**, 2012, pp. 311–330 (doi: 10.1177/0021998311424624).

[8] M. Irfan, V. Machavaram, R. Murray, F. Bogonez, C. Wait, S. Pandita, M. Paget, M. Hudson and G. Fernando, The design and optimisation of a rig to enable the lateral spreading of fibre bundles, *Journal of Composite Materials,* **15**, 2014, pp. 1813–1831 (doi: 10.1177/0021998313490770).

[9] M. Belhaj, M. Deleglise, S. Comas-Cardona, H. Demouveau, C. Binetruy, C. Duval and P. Figueiredo, Dry fiber automated placement of carbon fibrous preforms, *Composites Part B: Engineering*, **50**, 2013, pp. 107–111 (doi: 10.1016/j.compositesb.2013.01.014).

[10] D. Lukaszewicz, C. Ward and K. Potter, The engineering aspects of automated prepreg layup: History, present and future, *Composites Part B: Engineering*, **3**, 2012, pp. 997–1009 (doi: 10.1016/j.compositesb.2011.12.003).

[11] Jeff Sloan, ATL and AFP: Defining the megatrends in composite aerostructures, *High-Performance Composites*, 4, pp. 68, 2008.